LONDON, METEOROLOGICAL OFFICE.

Met.O.15 Internal Report No.64.

Air flow and precipitation distribution within a cloud signature seen on satellite imagery associated with a developing mid-latitude depression. By YOUNG,M.V.

London,Met.Off.,Met.O.15 Intern.Rep.No.64 1986,31cm.Pp.22,17 pls.6 Refs.Abs.p.2.

An unofficial document - not to be quoted in print.

METEOROLOGICAL OFFICE
London Road, Bracknell, Berks.

MET.O.15 INTERNAL REPORT

No. 64

Air flow and precipitation distribution within a cloud signature seen on satellite imagery associated with a developing mid-latitude depression.

by

M. V. Young

Jan 1986

Cloud Physics Branch (Met.O.15)

LF/M015

Contents

Summary

A cyclone which crossed southern Britain during 20 September 1984 was accompanied by a baroclinic leaf cloud which evolved into a comma shaped cloud system. Detailed interpretation of satellite and radar imagery, as well as synoptic observations is carried out in order to identify the major airflows within the evolving cloud system and to study the relationship of these airflows to the observed precipitation distribution. Several aspects of this development as observed in the satellite imagery are identified as being potentially useful in forecasting.

1. Large scale evolution

Three stages in the life cycle of the cloud mass associated with the cyclone in this study are shown in the NOAA7 infra-red images Fig. 1a-c. The cloudmass lay in a baroclinic zone and is labelled 'B'. It was initially an elongated feature with tops aligned roughly west-southwest to east northeast. Hourly METEOSAT images (not shown) suggest that during 19 September this cloud mass had been translating eastwards with little significant change of shape. Adjacent to its northern flank, in the cold air, was a mass of lower cloud tops labelled C.

Late on 19 September and during the 20th, this whole cloud mass, as depicted by the high cloud tops began to rotate cyclonically until by the afternoon of the 20th (Fig 1c), a well-marked comma shape had emerged. By this time the rearward upper cloud boundary had overtaken the surface cold front (SCF) of the cyclone. The adjacent cloud area C in the cold air moved east with the main cloud mass B and became part of the comma pattern evident in the high cloud. Meanwhile, cloud dissipation occurred on the southern tail of the comma.

The whole cloud mass, B, as shown up by the high cloud tops will be referred to as a 'baroclinic leaf' after Weldon (1979). (Weldon introduced this term to refer to the characteristic leaf-shaped cloud pattern often observed in satellite imagery during the early stages of development of a mid-latitude cyclone)

Figures 2a-c show schematically the cloud outlines at 12 hourly intervals starting at 12Z 19 September. These have been derived from both METEOSAT and NOAA7 imagery. The location of jet streams and surface fronts are superimposed.

Associated with the baroclinic leaf, B, was a wave depression labelled LG. Surface hand analyses showed LG to be running east at 35-40 knots during 19 September, but by 12Z 20 September it had slowed down to nearer 25 knots. Its central pressure fell by 11 mb in the 24 hours until 12Z 20 September and dropped by several more millibars as it ran eastwards over the North Sea. Numerical model analyses were used to supplement the sparse data around LG whilst it lay over the ocean.

LG tracked eastwards initially beneath the right hand entrance region of a jet streak labelled J1, the northern edge of B remaining parallel to the axis of J1 (Figure 2a and b). During the morning of 20 September both the rearward edge of B and the axis of J1 overran the surface cold front and by 12Z 20 September LG lay beneath the left-hand entrance region of J1 (Fig 2c). Therefore LG was no longer in a favourable development area. Upstream, a jet streak labelled J2 was propagating eastwards. However J2 and its associated cloud (not shown) remained separate from both LG and J1, and had little effect on LG's subsequent behaviour. This factor distinguishes this case study from that of 26 November 1983 (Young, Monk, Browning (1985)) in which the upstream jet streak contributed to the rapid deepening of a surface depression.

Unlike the 26 November 1983, there was no evidence of stratospheric air with high potential vorticity (PV) being injected from upstream into middle and upper levels of the cyclone in question. High PV air, present to the north of J2 remained separate from LG, although there was an axis of maximum PV (dot dashed line in Figure 2) lying along the weak upper trough behind LG.

Fine mesh numerical model output is used in this study as a diagnostic tool for inferring aspects of the meso and synoptic scale dynamics of the cloud system. Figure 3 shows forecast sea level pressure and rainfall rates at 6 hourly intervals from the operational fine mesh model data time 12Z 19 September 1984. Use of the model is justified in that until T+18 the predicted pressure and rainfall distribution compare well with reality (see Figure 2) although the eastward movement is rather too quick. However, by T+24, 12Z 20 September the model has lost the circulation around LG. This problem was also present in the fine mesh forecast based on data 12 hours later. Forecasts of the upper air pattern (not shown) were generally good, likewise the overrunning process as modelled in the humidity fields.

2. Developments during the period 03Z-15Z 20 September 1984

(a) Baroclinic leaf and dry intrusion

This is the period during which the baroclinic leaf was rotating cyclonically with its tail progressively overrunning the surface cold front giving rise to a 'split-cold front' structure (Browning and Monk (1982)). The process is demonstrated in Figs. 4a and b. Water vapour imagery, Figure 5, which is sensitive to the presence of moisture in the mid and upper tropopshere showed dry air lying immediately behind the leaf. In Figure 5 the driest air shows up as white and the moistest as black, the dry air being labelled 'D'. The distinct forward edge of this dry air is shown schematically as a heavy line in Figure 4b, and will be referred to as the 'upper cold front' (UCF) as defined by Browning and Monk (1982). This dry zone appears similar to the 'dry intrusion' referred to by Young et al 1985 (26 November 1983 case) except that in this instance there is no evidence of

stratospheric air extending to such low levels as in the November 1983 case (as inferred from the PV distribution). However this dry air substantially modified the precipitation distribution and cloud pattern as it overran the surface cold front and depression centre.

Considerable convective cloud growth took place in cloud area C during the period 09Z to 12Z after the UCF had overtaken the SCF. The convective tops are clearly visible on Figure 1c. Meanwhile, the upper cloud along the tail of the leaf was dissipating, model products suggesting subsidence aloft in that region.

(b) Rainfall distribution

(i) Preoverrunning

The preoverrunning stage refers to the stage of development of LG until 06Z when the rear edge of the upper cloud overtook the SCF.

Combined synoptic and radar observations show that rain was falling from a large proportion of the leaf (up to 70% of its area at 05Z). Particularly noteworthy is the extensive area of heavy rain with embedded thunderstorms which was present near the warm front over southern Britain. Radar derived rainfall rates (calibrated in real time using raingauges) showed rates in excess of 8 mmh^{-1} over a large area. This area of heavy rain was already well-developed by 00Z 20 September when the rain first came within the range of Clee Hill radar and persisted until late morning, tracking eastwards, associated with a minor wave on the warm front. In view of the potential instability present in the Camborne and Larkhill ascents (Figs 6a and b) and the upward motion suggested by the model over southern England (Fig 7) this

rain area was probably a mesoscale convective system being fed by potentially unstable warm low level air rising over the warm frontal zone.

(ii) Post overrunning

ii.1 Significance of the split front

Once the dry intrusion to the rear of the baroclinic leaf had overtaken the SCF, a split-front formed. (Browning and Monk, 1982, Young et al, 1985)). The UCF is preceded by layered cloud up to around 300 mb as suggested by METEOSAT derived cloud top temperatures of around -40°C and the Hemsby ascent, Fig 6c. Between the UCF and SCF lies a shallow moist layer of high θ_w surmounted by dry air. This is demonstrated on the Crawley ascent (Figure 6d) in which the dry air is present above 700 mb, and is labelled 'D'. Successive water vapour images suggest that this dry air has originated to the rear of LG.

Rainfall which had been largely continuous on and ahead of the UCF became more intermittent and lighter in the region between the UCF and SCF owing to a much shallower depth of cloud. However, potential instability was present within this region as indicated by the Crawley ascent. A SFLOC report at 13Z over SE England as well as surface based observations of large cumulus suggested that some deep convection did occur, and there were further SFLOCS reported over the near continent later in the afternoon ahead of the SCF. These were confined to the area of largest pressure falls near the depression

centre where large scale bodily ascent would be expected. Additionally some breaks developed in the low cloud away from exposed coasts ahead of the SCF allowing surface temperatures to rise to 17°C in parts of southeast England. This combined with dewpoints of 14°C would, on the basis of the Crawley ascent, lead to deep convection.

ii.2 Development of precipitation within the cold air

In this section we concentrate upon the development of precipitation from the mass of cloud labelled C, within the cold air. Until 08Z this feature had remained relatively unchanged in terms of its extent and cloud top temperature (see Figure 4). This lay between 0°C and -10°C which when correlated with nearby ascents gave cloud tops of around 650 to 700 mb. As yet little or no precipitation fell from C. However, between 09Z and 12Z (Fig 4a) considerable cloud growth took place in C with tops soon rising to 400 mb (around -35°C). This was accompanied by precipitation development, with evidence of some heavy rain by midday and SFLOC reports in the afternoon over East Anglia.

The above transition was reflected in the water vapour imagery. The dry air which had overlain C for some time before overrunning commenced became much moister in that region between 09Z and 12Z through deep convection and is labelled 'M' on Figure 5.

Two soundings which give perhaps the closest representation of area C are Valentia at 00Z and Aberporth at 06Z 20 September (Figs 6e and f). A marked dry, stable layer above 700 mb at Valentia would act to inhibit any mid-level convection. However, at Aberporth potentially unstable air is present at 06Z due to the introduction of high θ_w air around 700 mb and advection of colder air above this level. Progressive destabilisation of the air in C was therefore occurring leading to the eventual development of convection. A fuller explanation of this process in terms of conveyor belts is presented and justified in Chapter 3.

(c) Surface synoptic developments

The aim of this section is to look in more detail at the synoptic developments as inferred from the surface observing network over Britain in relation to model diagnostics and satellite imagery.

Several aspects of this cyclonic development are worthy of note. Until overrunning occurred, the centre of LG lay near the inflection point towards the rear of the leaf. The surface pressure pattern associated with LG was complex. A marked trough in the pressure and wind fields extended to the east and northeast of LG beneath the upper level cloud shield. This trough had been present since 18Z 19 September and within it was at least one minor circulation which could be tracked over a 15 hour period moving with approximately the same velocity as LG.

The development of the split front as seen from a time sequence of surface observations is shown in Figure 8. Figure 8 can be used in conjunction with Figure 4b, on which the locations of the observing stations chosen are superimposed upon the cloud pattern. These are Scilly Isles (Sc), Boscombe Down (Bo), Heathrow (H), and Manston (Ma). The SCF was well marked as it entered southwest England, crossing the Scilly Isles between 5Z and 6Z 20 September exhibiting almost coincident changes in wind direction, dewpoint, and cloudbase as well as a sharp pressure kick. This is labelled 'L' on Figure 8. At this stage (see Figure 4b) overrunning had not yet occurred. However, by the time that the SCF had reached Boscombe Down, that is, at around 12Z (labelled 'M' on Figure 8) overrunning had taken place. The passage of the UCF between 10Z and 11Z was marked by cessation of the heavy rain accompanied by a rise in the cloudbase along with a temporary halt in the pressure fall. A similar sequence of events was observed at Heathrow and Manston, the passage of the UCF being labelled 'U' on Figure 8. At Heathrow, large cumulus was reported at 13Z immediately after passage of the UCF, this convective cloud development occurring within an area of potential instability referred to in section 2(b)(ii).1. The arrival of cold air at the surface at Heathrow and Manston did not take place with the passage of the SCF, but instead on a minor trough that was forming immediately behind the SCF. (This trough is shown on Figure 4 as a solid line stretching southwest from the main depression centre). In Figure 8 we see at Manston the passage of the UCF at U, the SCF at S, and the trough at T. The trough which probably coincided with the axis of the upper air trough was not evident on satellite imagery.

Figure 9 shows the main surface features over the British Isles at 00Z, 06Z and 12Z 20 September. Superimposed as a dot-dashed line is the thermal front parameter, TFP. (Zwatz-Meise and Hailzl, 1983). This is defined as

$$TFP = \max \left\{ -\nabla \left| \nabla T \right| \left(\frac{\nabla T}{\left| \nabla T \right|} \right) \right\}$$

It represents the maximum change of thickness gradient ∇T in the direction of the thickness gradient, and can therefore be used to locate fronts present within the chosen layer, in this case 850/500 mb. Moreover, this parameter is defined so as to place the front on the warm side of the thickness gradient. The TFP has been extensively used by Zwatz-Meise in conjunction with satellite imagery to establish whether or not a band of cloud is associated with a front. In addition to the TFP, the outline of cloud leaf B is shown in Figure 8.

The warm front labelled F1, (Figures 9a and b) north of which the MCS developed (described in Chapter 2(b)(i)) is not associated with a maximum of TFP. However, since the front is evident in model 1000/850 mb thickness fields (not shown) F1 is therefore only of limited vertical extent. Progressively, surface observations during the morning of 20 September showed that the elongated trough labelled F2 was assuming frontal characteristics. Indeed, the TFP showed that this trough had been associated for some time with a deep frontal zone. By 12Z F2 had taken over as the dominant warm frontal zone both at the surface and aloft.

The TFP to the rear of LG does not coincide with any upper cloud, and always lies well behind the SCF. The absence of cloud is consistent with model products which show dry air and subsidence aloft within the frontal zone as defined by the TFP. Further studies will be necessary to establish the usefulness of the TFP.

3. Conceptual model

Conceptual models have been derived for this cloud system corresponding to the pre-overrunning stage, Fig 10a, and the post overrunning stage, Figure 10b. These correspond to around 05Z and 12Z respectively. The models have been derived by combining satellite, radar, and synoptic observations, as well as numerical model diagnostics. Evidence for the derived flow configurations is presented at the end of this section.

In Figure 10a, the pre-overrunning stage, two major flows are readily identified.

(1) The warm conveyor belt flow labelled W1 gives rise to the observed cloud leaf. This air contains pockets of potential instability and the instability is released giving the area of heavy rain and thunderstorms (referred to in Section 2(b)(i)) as it rises over warm frontal zone F1 (Fig 9b).

(2) The flow of dry air (labelled D) to the rear of the leaf. The forward boundary of the dry air (the upper cold front) is marked as a bold double line. This is inferred from the water vapour imagery. In addition, a cold conveyor belt flow (Carlson, 1980) appears to exist below 700 mb, that labelled C1 associated with cloud mass C.

In Fig 10b, some time after overrunning has occurred, we see the flows W1 and D, and C1 already referred to in Figure 10a. (C1 is not shown on the diagram). However, in the zone between the upper cold front at the forward edge of D, and the surface front, we have a shallow moist zone beneath the dry air. Although this flow is really part of W1, we shall refer to it as a second warm conveyor belt W2 which also ascends over the warm front. Being situated beneath the dry air, potential instability is released as W2 ascends and this is thought to have given rise to the development of convective rain in area C represented by plus signs in Figure 10b.

Observed rainfall distributions are shown as shading in Figure 10. Large scale ascent gives rise to rainfall beneath much of the leaf, dying out under its northernmost portion. Precipitation is generally intermittent and more drizzly in nature between the UCF and SCF, except near the depression centre where large scale ascent releases potential instability giving rise to convective outbreaks.

Evidence is presented below for the various airflows depicted in Figures 10a and 10b.

W1

There is a similarity in appearance between the leaf in this case study and that of 26 November 1983 (Young et al, 1985). Therefore as a first guess, one can assume a similar internal flow regime.

Winds calculated from the 06Z ascents and model forecasts relative to 270/40, which is the assumed motion vector for the leaf, show that upper level air is flowing roughly parallel to the rear edge of the leaf.

Model ω fields, an example of which is shown in Figure 7, suggest an area of upward motion throughout much of the troposphere corresponding to the observed leaf.

There is a southwesterly jet associated with the leaf, located around 300 mb.

Water vapour imagery (Figure 5) shows progressive moistening at upper levels from the tail to the head of the leaf, suggesting upward motion of air flowing through the leaf.

W2

A low level jet is present in the 12Z Crawley ascent, Figure 6d, within a warm moist air mass extending up to 700 mb suggesting that a warm conveyor belt exists (Browning and Pardoe, 1973). The Aberporth 06Z ascent, Figure 6f, has high θ_w air at around 700 mb exhibiting a southerly flow relative to the motion of LG, taken to be 260/25. This is a shallow flow, lying between two layers of air with lower θ_w.

D

This flow is evident on water vapour imagery as the area marked D on Figure 5, and also in the radiosonde ascents as a dry layer, for example Valentia 00Z, Aberporth 06Z, and Crawley 12Z 20 September. The layers referred to are all marked with a D on Figure 6. Model humidity fields (not shown) also reveal this tongue of dry air.

C1

The Aberporth 06Z ascent, Figure 6f, exhibits a low level northerly jet with a reported wind of 010/26. Relative to the motion of LG Valentia 00Z, Figure 6e, has a northeasterly flow at around 850 mb.

4. Identification of possible forecasting aids and areas requiring further study

In this section a summary is presented of the more significant findings of this case study and their possible implications in forecasting. All of the following features have also been observed to occur in other cases of cyclogenesis studied, (eg 26 November 1983, 11 April 1985) although not necessarily altogether in each particular case.

1. During cyclogenesis a baroclinic leaf cloud emerged from a straight edged mass of high cloud.

2. Once formed, rotation of the leaf took place. This may be indicative of cyclogenesis, although as this case demonstrates, rotation does not necessarily imply rapid cyclogenesis.

3. Water vapour imagery appears useful for observing overrunning of the surface cold front by the upper cold front with its accompanying modification of the precipitation pattern.

4. Until overrunning, the surface wave or cyclone lay near the inflection point towards the rear of the leaf.

5. Rainfall developed and intensified in the cold conveyor belt (comma head) area within several hours of overrunning.

Listed below are some important areas requiring further study.

1. In this case study rainfall occurred under a large proportion of the leaf. Further studies will be necessary to determine whether or not this is a common feature of baroclinic leaves.

2. We need to examine further the relationship between rotation of the baroclinic leaf and the overrunning process, in particular the length of time separating these two events, and also how they relate to the onset of rapid cyclogenesis in some cases.

3. Jet streaks have been shown to influence the rate of cyclonic development in this and other case studies. In the cases of 26 November 1983 and 11 April 1985 rapid cyclogenesis has been attributed to large scale dynamically forced ascent near the left hand exit of a jet streak, an area where air of high potential vorticity (PV) is being injected into the cyclonic circulation. However, on 20 September 1984 when cyclogenesis was much less intense, no such dynamical processes existed in the vicinity of the cyclone. Clearly this is an area requiring further study, and the role of PV must be clarified through more case studies.

4. The role of the thermal front parameter and its relation to cloud and rainfall distribution is as yet uncertain and merits further investigation.

Figure Captions

Figure 1

NOAA7 infra-red images for:

a. 1509Z 19 September 1984

b. 0513Z 20 September 1984

c. 1456Z 20 September 1984

The baroclinic leaf is labelled B. C is a cloud mass in the cold air adjacent to B and has lower, warmer tops.

Figure 2

Surface fronts, depression centres, jet axes, and cloud boundaries for

a. 12Z 19 September 1984

b. 00Z 20 September 1984

c. 12Z 20 September 1984

Depression centres are denoted by a cross alongside the central pressure in millibars. Jet axes at 300 mb are shown by bold solid lines labelled J1 and J2, with isotachs marked as thin lines labelled in knots. In Figures (b) and (c), the horizontally hatched area within a solid line shows cloud with tops colder than -30°C, and the area with pecked hatching within a dashed line shows cloud with tops in the range 0°C to -30°C. In (a) the approximate distinction between the two ranges is given by the difference between warm (dark) tops and cold (bright) tops as derived from NOAA7 imagery. The baroclinic leaf is labelled B, and the cloud mass in the cold air, C. Axes of maximum potential vorticity on the 330°K surface are shown as dot-dashed lines.

Figure 3

Operational fine mesh forecast, data time 12Z 19 September 1984, up to 24 hours. Fields of sea level pressure and rainfall rate are shown at 6 hourly intervals starting at 18Z 19 September. The symbols denoting rainfall are defined in the figure. The depression being studied is approaching southwest Ireland at 18Z 19 September.

Figure 4

Schematic representation of surface fronts, cloud, and rainfall distribution at 2 hourly intervals for the period 03Z-15Z 20 September 1984.

In Figure 4(a) horizontal hatching corresponds to cloud tops colder than -30°C. Dashed lines show boundaries of the cloud with tops colder than 0°C, the temperatures being deduced from METEOSAT imagery. The extent of rainfall as deduced from surface observations and radar coverage is shown by the sparsely stippled area within a thin continuous line. Areas of heavy rainfall (greater than 4 $mmh^{-1)}$ are densely stippled. C is the area of cloud within the cold air.

In Figure 4(b) the heavy black line represents the boundary of the dry air aloft derived from water vapour imagery. The rainfall distribution is omitted in Figure 4(b). The locations of various observing stations are superimposed upon the cloud pattern in each diagram. These are Scilly Isles (Sc), Boscombe Down (Bo), Heathrow (H), and Manston (Ma).

Figure 5

METOESAT water vapour imagery at 3 hourly intervals for the period 03-15Z 20 September 1984. This is most sensitive to moisture around 400 mb. White areas represent the driest air and black the moistest. The moisture associated with the baroclinic leaf is clearly visible, likewise

the flow of dry air labelled D, to the rear of the leaf. M denotes the area in which moistening of the air at upper levels is taking place due to deep convection.

Figure 6

Tephigrams and standard level winds for various stations on 20 September 1984

a. Camborne 00Z

b. Larkhill 06Z

c. Hemsby 12Z

d. Crawley 12Z

e. Valentia 00Z

f. Aberporth 06Z

Potential instability is present at Camborne (a) between 700 mb and 450 mb and at Larkhill (b) between 850 mb and 500 mb. Hemsby (c) lies in the deep layer of moist air ahead of the UCF. Crawley (d) shows the layer of dry air above 700 mb which has overrun the surface cold front and the moist layer beneath this level ahead of the surface cold front. Potential instability is present within this ascent, and the winds show cold advection within the dry air behind the UCF enhancing the destabilization. The layer of dry air corresponding to that which is present on water vapour imagery is labelled D on the appropriate ascents. Valentia (e) and Aberporth (f) both lie to the north of the depression centre within the region of dry air aloft. Note the presence of high θ_w air near 700 mb at Aberporth rendering the air potentially unstable. The superadiabatic lapse rate present at the top of the moist layers in Figs a, d and f is due to a

radiosonde problem that is frequently observed in the transition between very moist and very dry zones in the vertical and can be considered spurious.

Figure 7

Vertical velocity fields at 700 mb for 06Z 20 September derived from an 18 hour fine mesh forecast. Numerical values are in cms^{-1}, positive quantities representing ascent, and negative representing descent. Areas of ascent are horizontally hatched, values of more than 5 cms^{-1} being stippled. The area of strong ascent over southern Britain extending southwest into the Bay of Biscay is associated with the baroclinic leaf and is about 2 degrees of longitude too far east due to positional error of LG in the model's forecast.

Figure 8

Hourly observations during 20 September 1984 from Scilly Isles, Boscombe Down, Heathrow, and Manston. The letters on the diagram are used as follows:

U marks the passage of the upper level cold front. L, M, and S mark the passage of the surface cold front, and T marks the passage of a post cold frontal trough.

Figure 9

Surface fronts, cloud boundaries and thermal front parameter for (a) 00Z, (b) 06Z, (c) 12Z 20 September 1984. The three discernible surface fronts are labelled F1, F2, F3. Cloud boundaries are defined as in Figure 2. The thermal front parameter, TFP, is defined as

$$TFP = \max \{-\nabla|T|(\pm\frac{\nabla T}{|\nabla T|})\}$$

and is shown as a dot-dashed line. In (a) and (b) the TFP is derived from 12 and 18 hour fine mesh forecasts, and in (c) is an analysis based on data from 12Z 20 September.

Figure 10

Conceptual model of the cloud system associated with LG showing relative flows, cloud and precipitation, (a) for the preoverrunning stage and (b) for the post overrunning stage. Diagram (a) corresponds to the system at around 05Z and (b) at around 12Z. The main cloud areas as observable on infra-red imagery are shown by horizontal hatching. The area of rainfall is stippled. Circles represent rainfall caused by large scale slantwise ascent of warm air, (dynamic rainfall) plus signs represent convective rainfall due to ascent of potentially unstable air, and commas represent drizzle. Bold arrows represent warm conveyor belt flows W1, W2 corresponding to the θ_w = 14°C surface, and dashed streamlines the flow of dry air, D, into the rear of the system. The forward edge of D is shown as a bold line, this being the upper cold front. W1 ascends from the boundary layer to near 300 mb giving rise to the leaf. The dot-dashed arrow is the cold conveyor belt flow labelled C1. W2 (Figure 9b) is that part of W1 which lies beneath the forward part of D, and ascends over C1 which is omitted from Figure (b) for clarity. The numbers indicate in millibars the approximate height of the various flows.

REFERENCES

Browning, K.A., and Monk, G.A. 1982:

A simple model for the synoptic analysis cold fronts. Quart. J. R. Met. Soc., 108, 435-452.

Browning, K.A., and Pardoe, C.W. 1973:

Structure of low-level jet streams ahead of mid latitude cold fronts. Quart. J. R. Met. Soc., 99, 619-638.

Carlson, T.N. 1980:

Air flow through mid-latitude cyclones and the comma cloud pattern. Mon. Wea. Rev., 108, 1498-1509.

Weldon, R.B. 1979:

Cloud patterns and the upper air wind field, Part IV. National Weather Service Satellite training notes, 80 pp. Unpublished manuscript available from Applications Division, National Earth Satellite Service, NOAA, US Dept. of Commerce.

Young, M.V., Monk, G.A., and Browning, K.A. 1985:

Interaction of a baroclinic leaf cloud and dry intrusion in a developing cyclone. Submitted to Quart. J. R. Met. Soc.

Zwatz-Meise, V., and Hailzl, G. 1983:

A cloud formation process contradictory to the classicial occlusion development investigated with satellite images and model output parameters.

Arch. Met. Geoph. Biocl., Ser. A, 32, 119-127 (1983).

Figure 1a

1509Z
19 September 1984

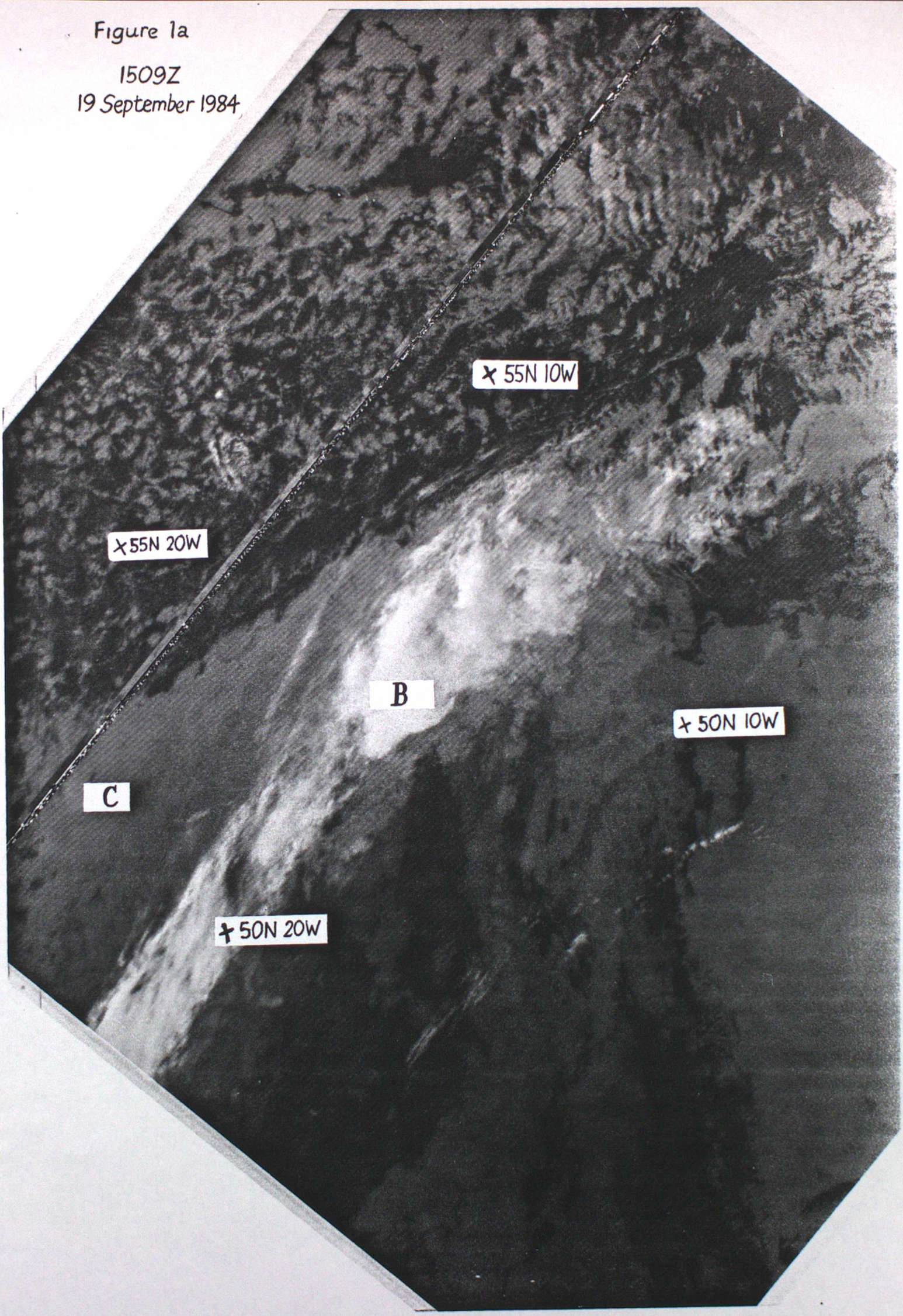

Figure 1b
0513Z
20 September 1984

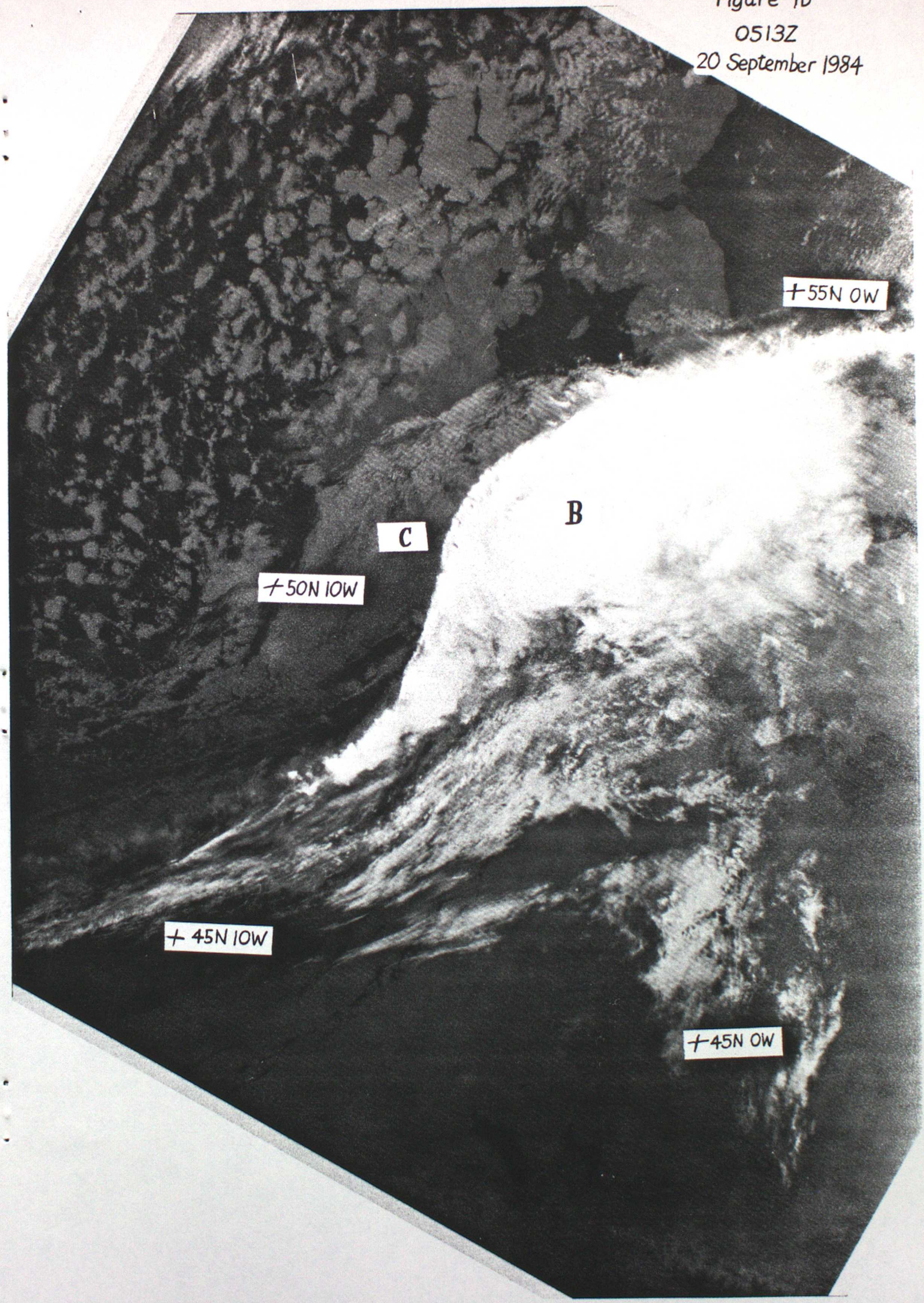

Figure 1c

1456Z

20 September 1984

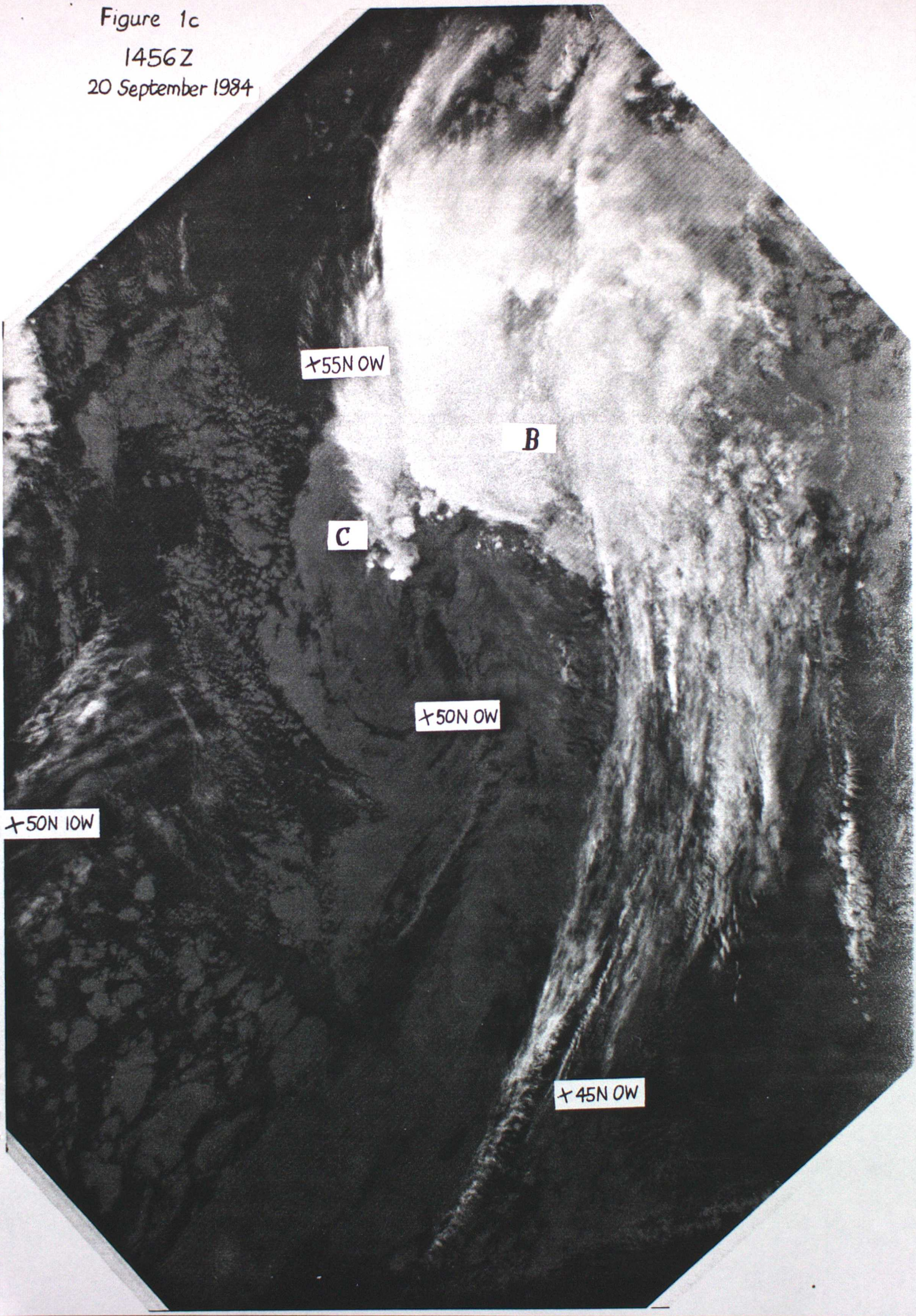

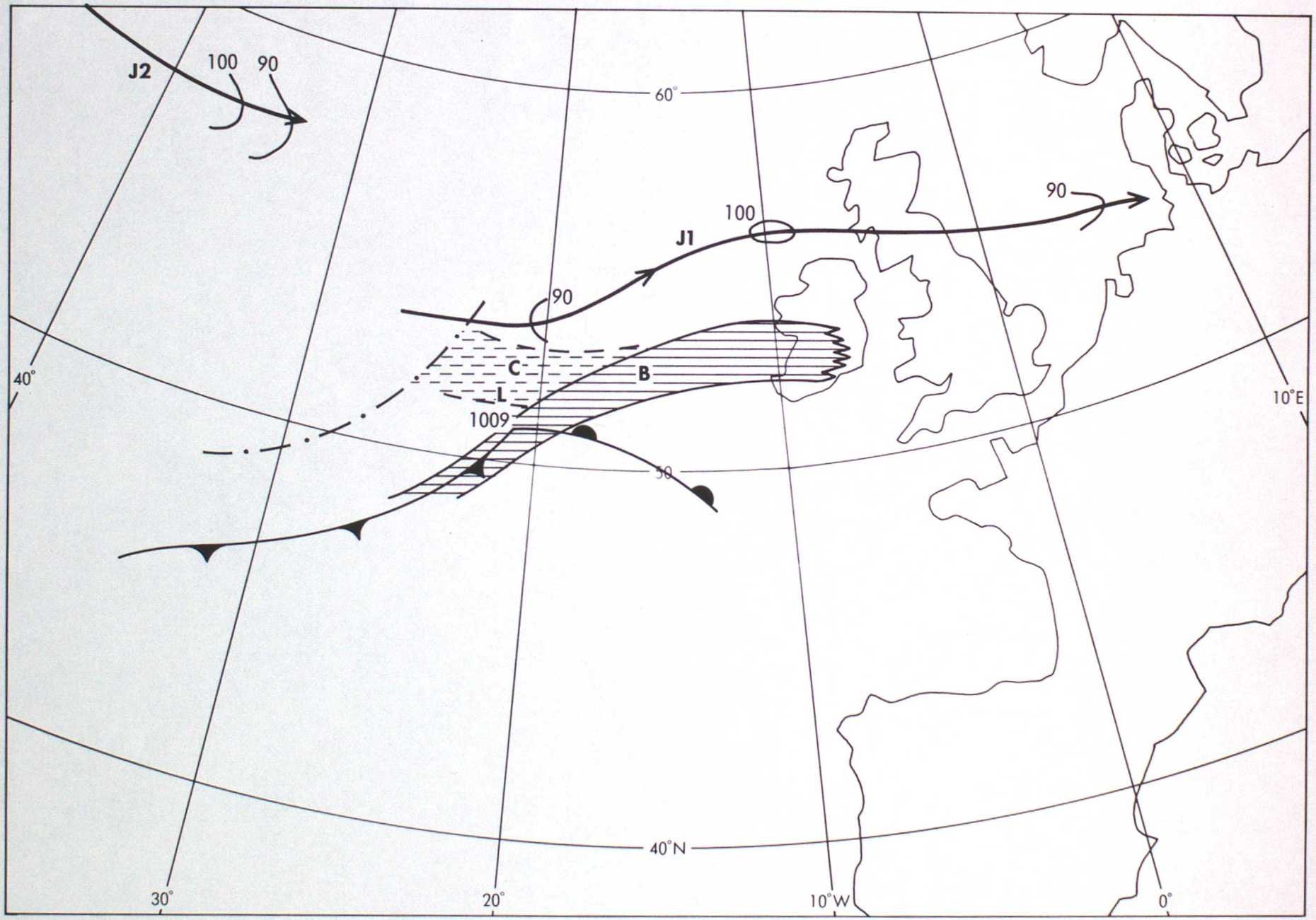

Figure 2a 12Z 19 September 1984

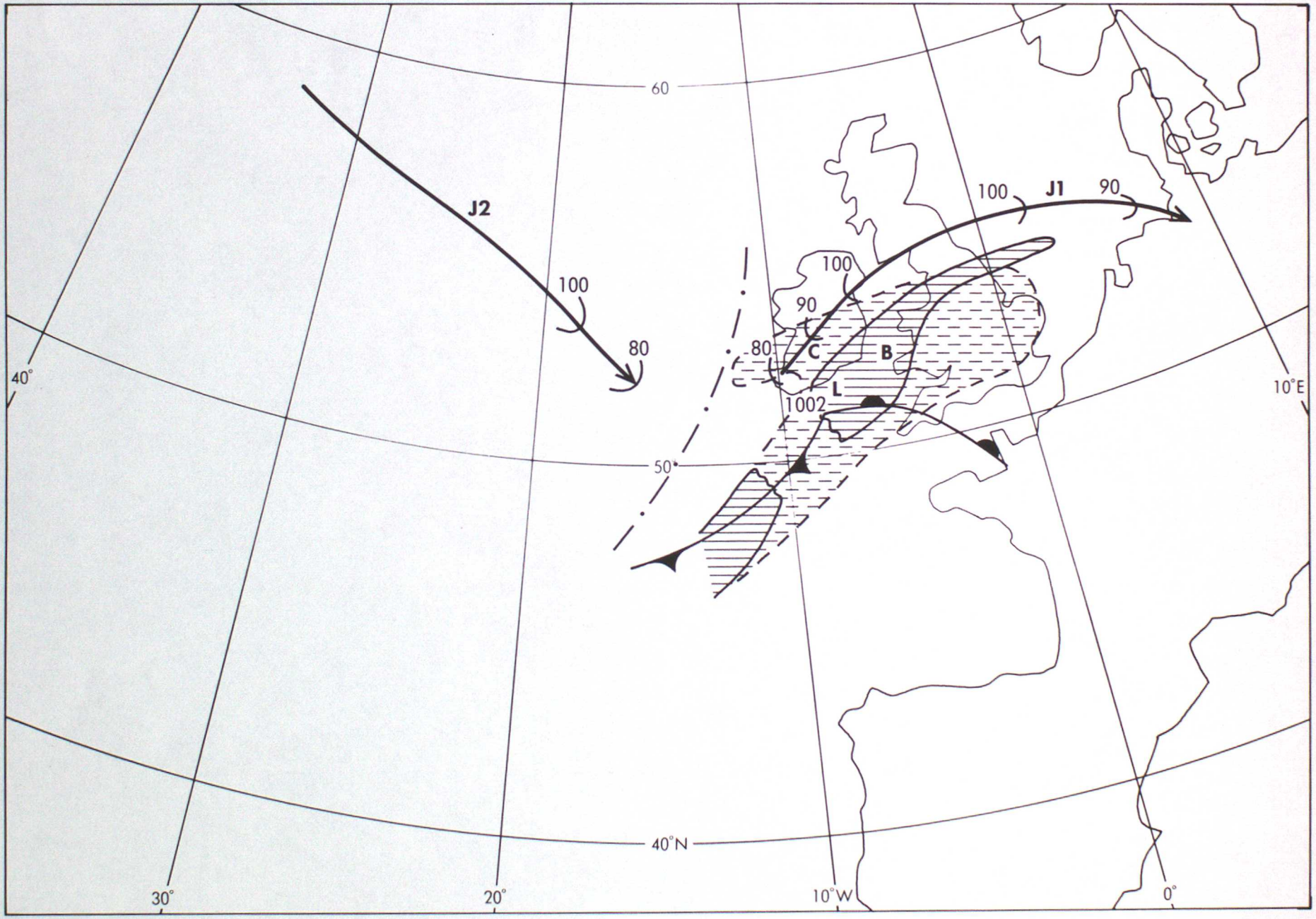

Figure 2b 00Z 20 September 1984

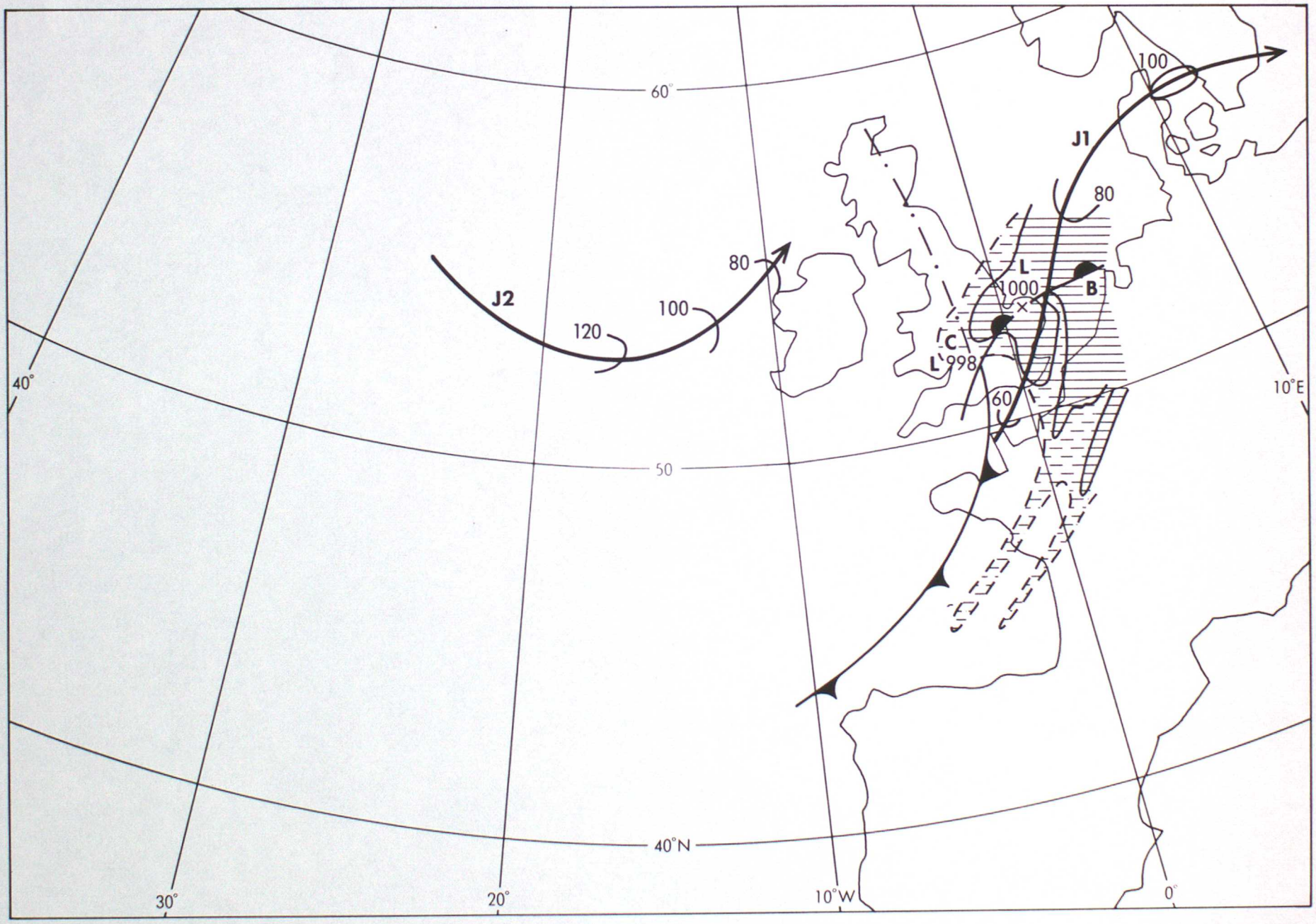

Figure 2c 12Z 20 September 1984

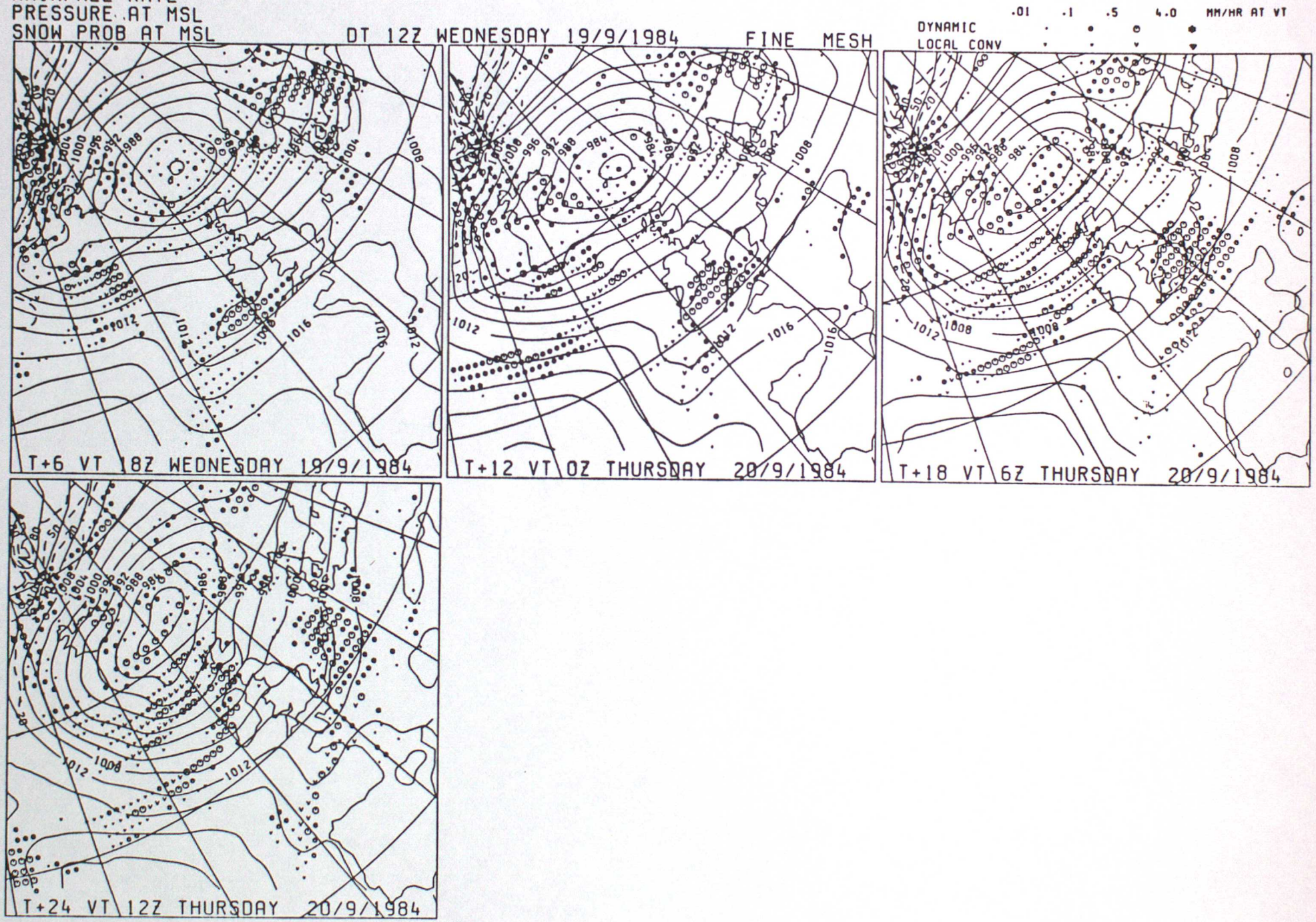
RAINFALL RATE
PRESSURE AT MSL
SNOW PROB AT MSL
DT 12Z WEDNESDAY 19/9/1984
FINE MESH
.01 .1 .5 4.0 MM/HR AT VT
DYNAMIC
LOCAL CONV
T+6 VT 18Z WEDNESDAY 19/9/1984
T+12 VT 0Z THURSDAY 20/9/1984
T+18 VT 6Z THURSDAY 20/9/1984
T+24 VT 12Z THURSDAY 20/9/1984

Figure 3

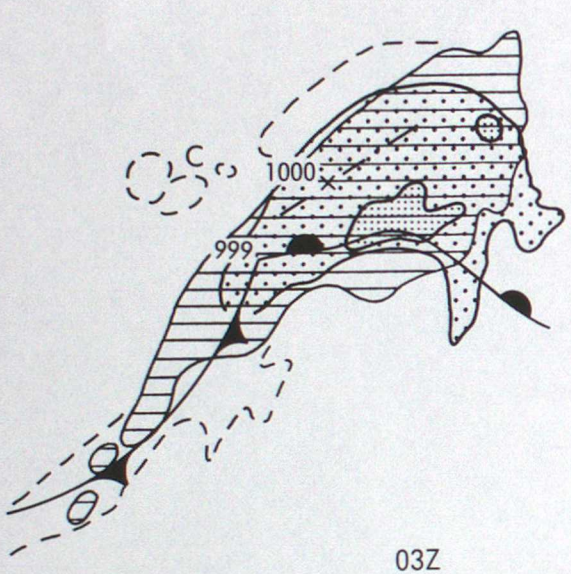

03Z

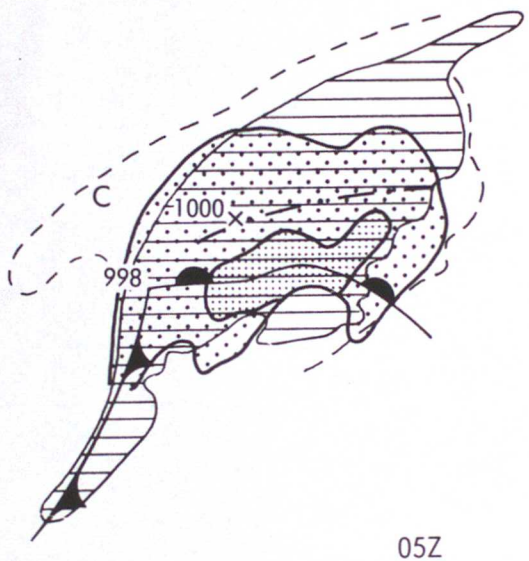

05Z

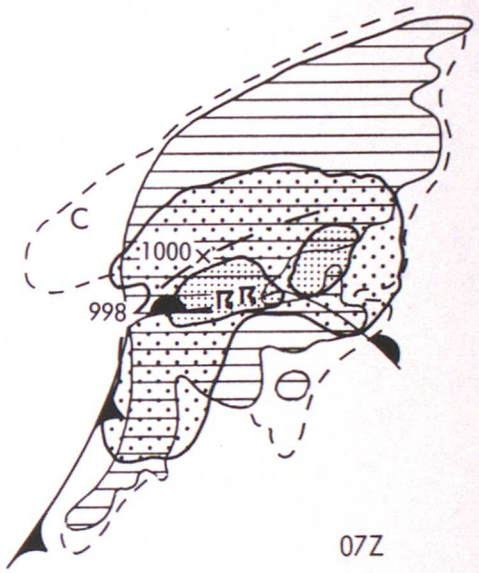

07Z

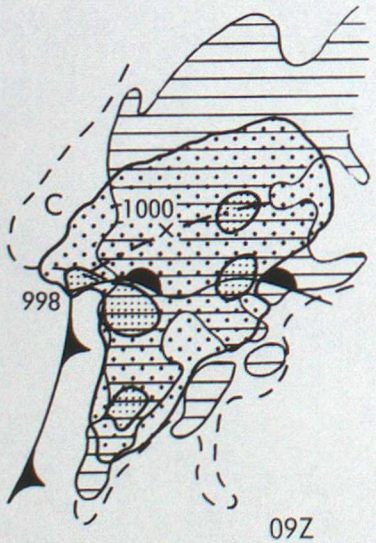

09Z

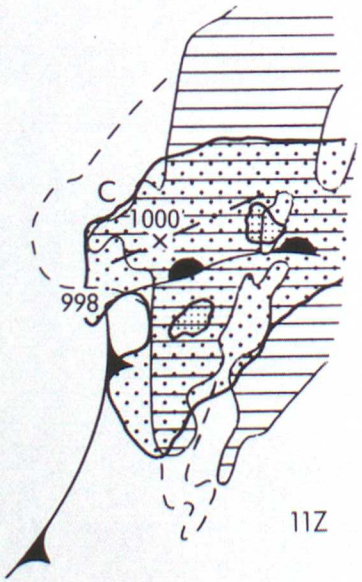

11Z

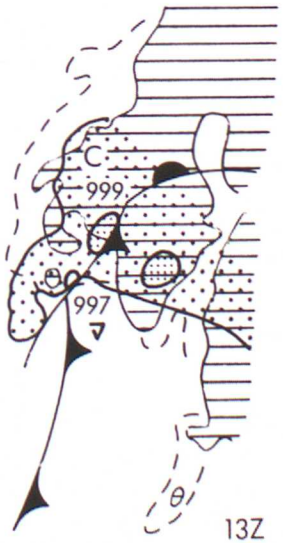

13Z

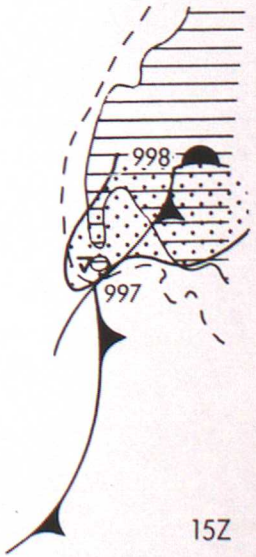

15Z

Figure 4a

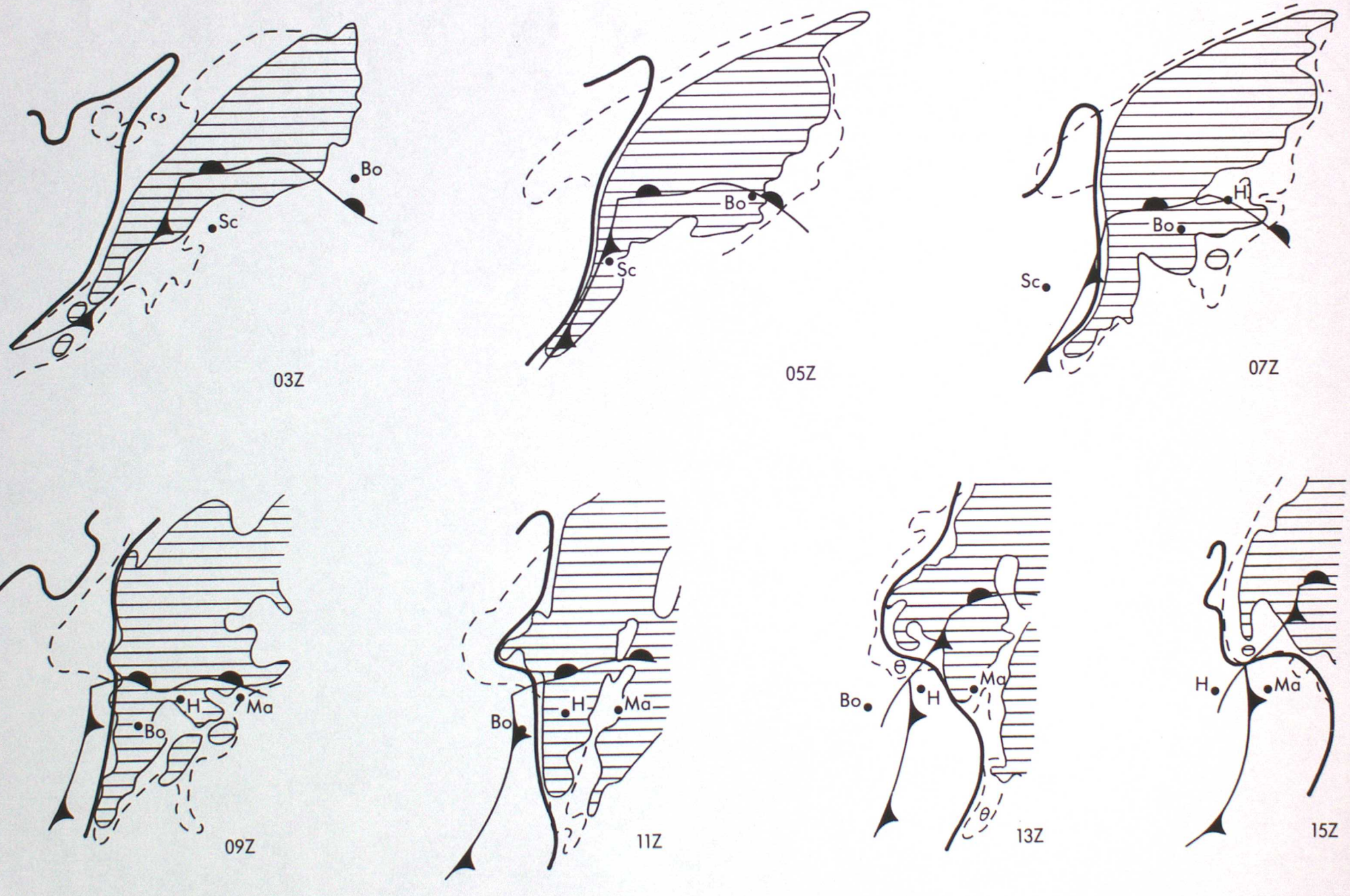
Bo
Sc
03Z
Bo
Sc
05Z
H
Bo
Sc
07Z
H
Ma
Bo
09Z
H
Ma
Bo
11Z
θ
Bo
H
Ma
θ
13Z
θ
H
Ma
15Z

Figure 4b

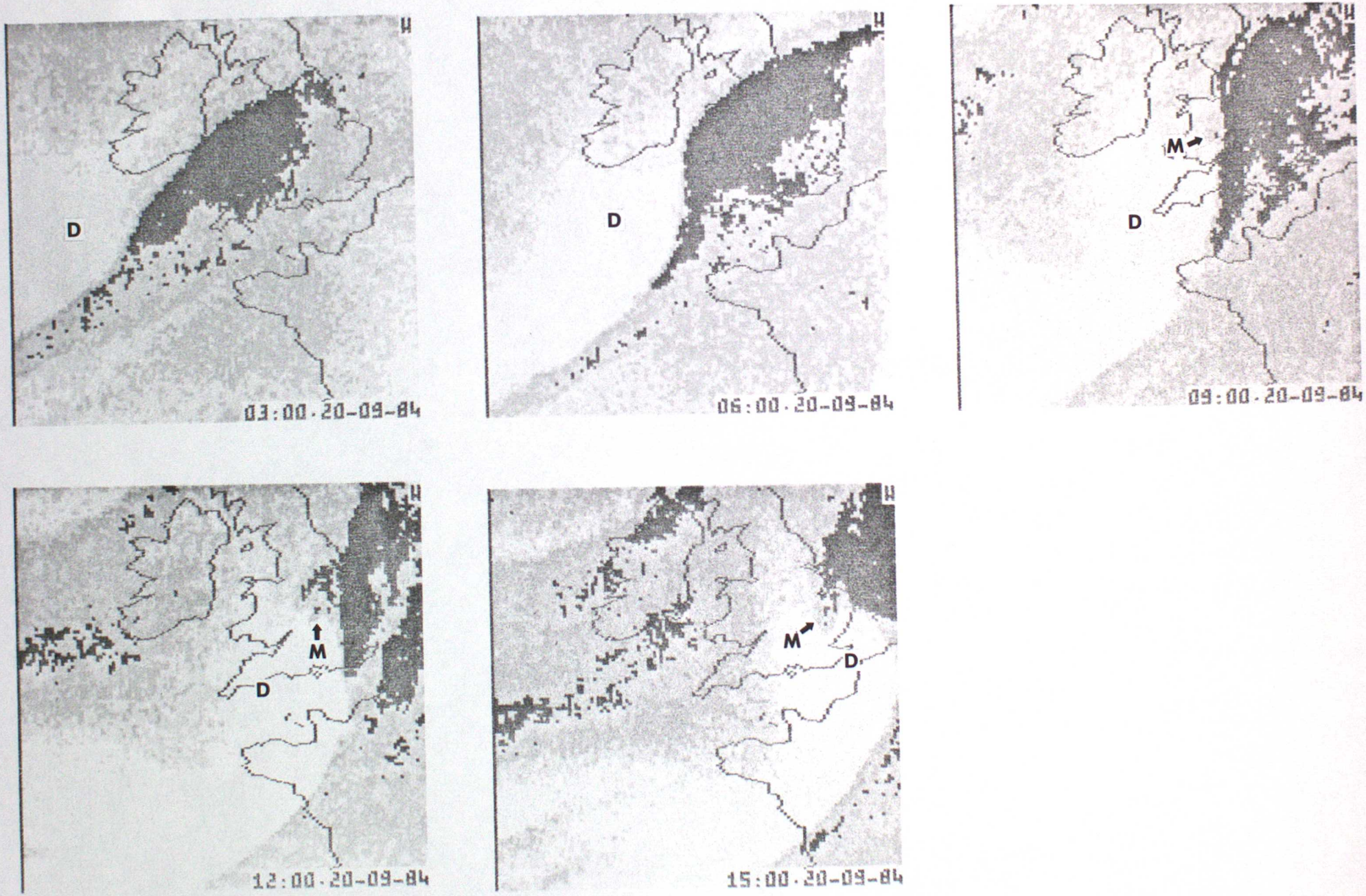
D
03:00·20-09-84
D
06:00·20-09-84
M
D
09:00·20-09-84
M
D
12:00·20-09-84
M
D
15:00·20-09-84

Figure 5

(a)

00Z

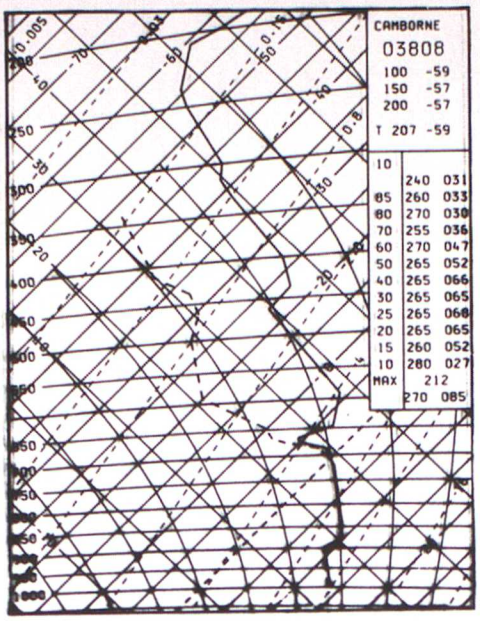

(b)

06Z

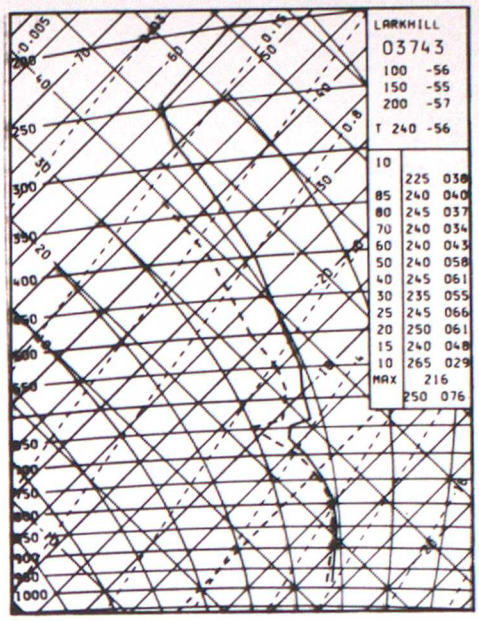

(c)

12Z

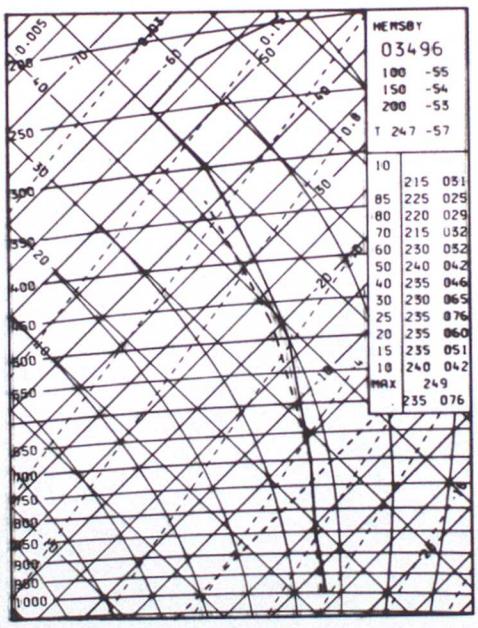

(d)

12Z

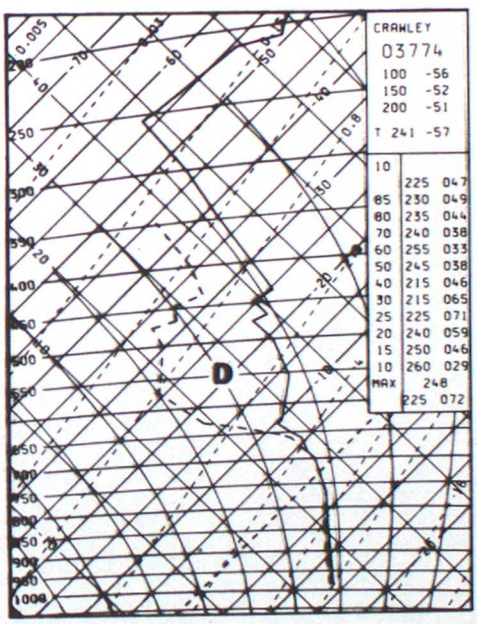

(e)

00Z

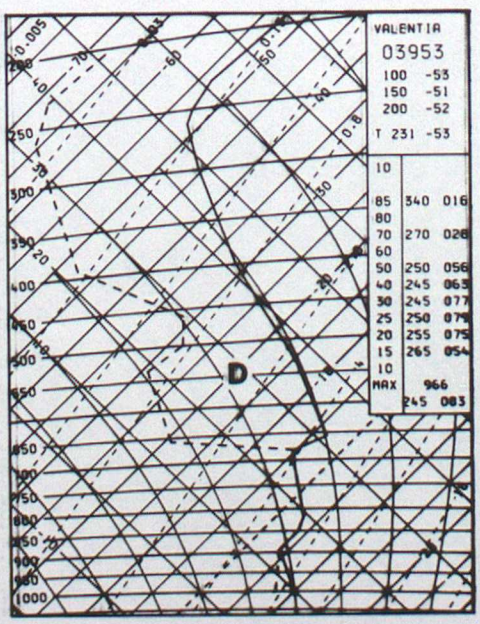

(f)

06Z

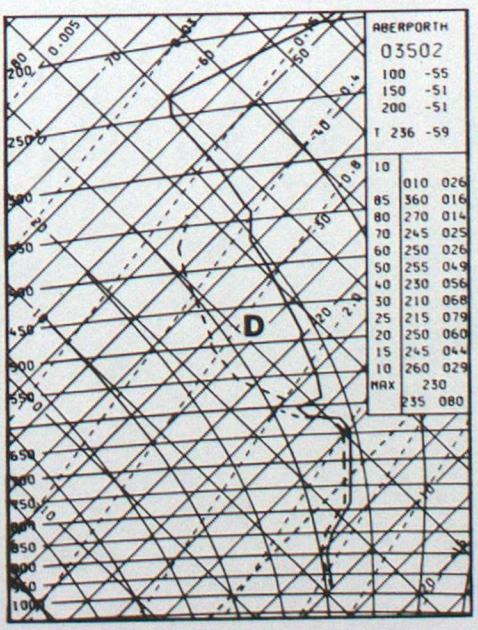

Figure 6

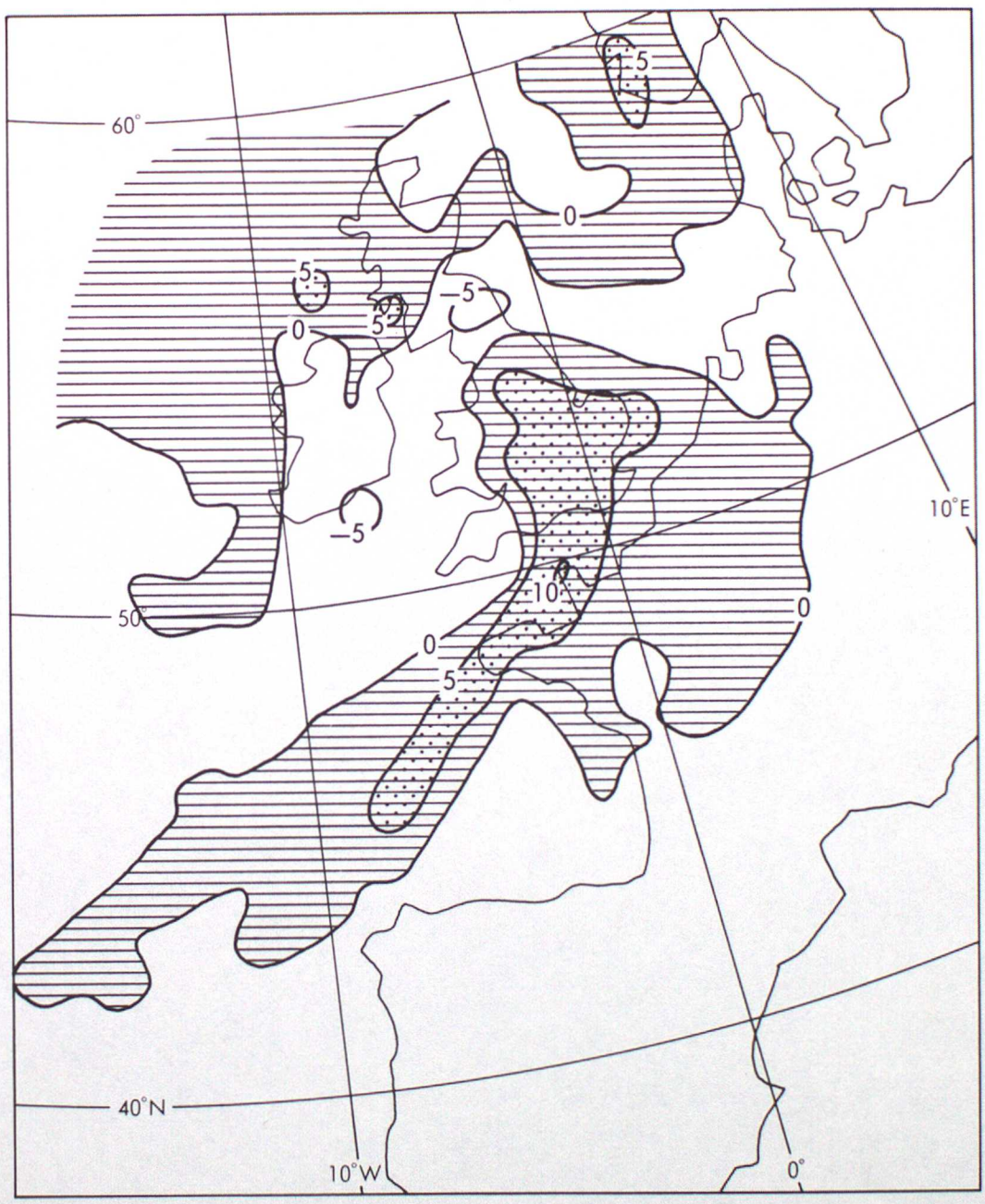

Figure 7

20 Sept. 1984 GMT	Scilly		Boscombe Down	Heathrow		Manston
03						
04			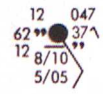			
05			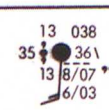			
06				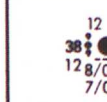		
07	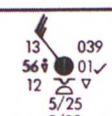			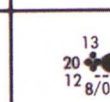		
08	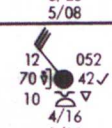		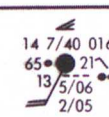	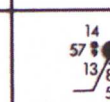		
09	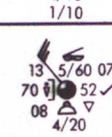		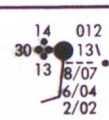	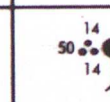		
10			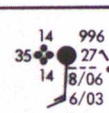	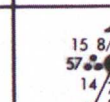		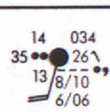
11			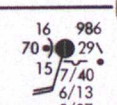	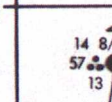		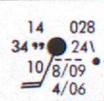
12			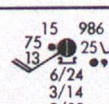	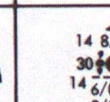		
13			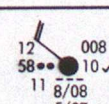	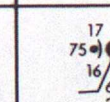		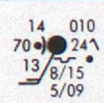
14			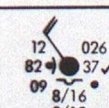	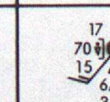		
15				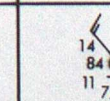		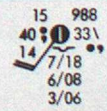
16				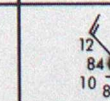		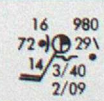
17						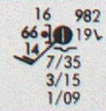
18						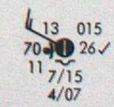

Figure 8

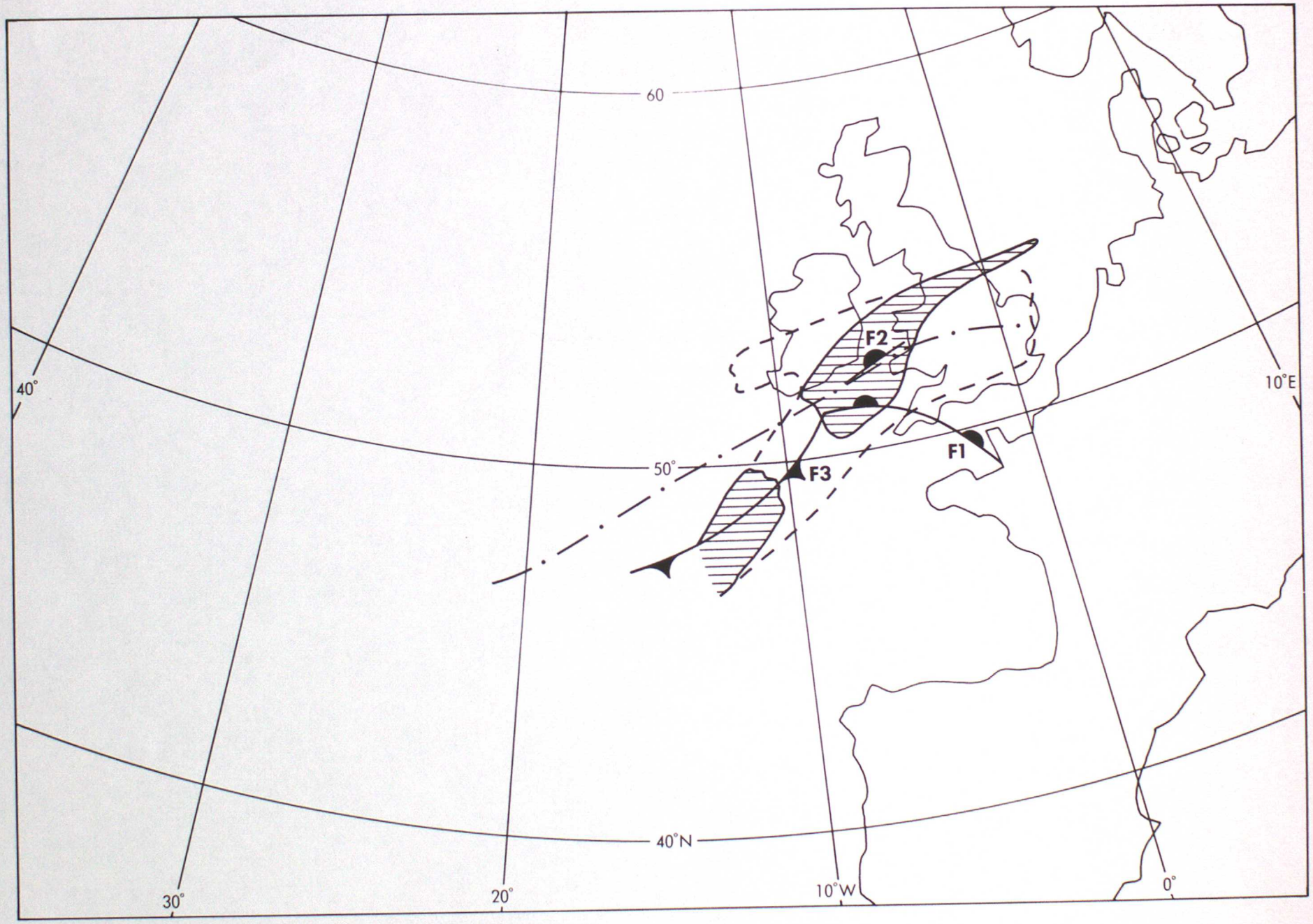

Figure 9a 00Z 20 September 1984

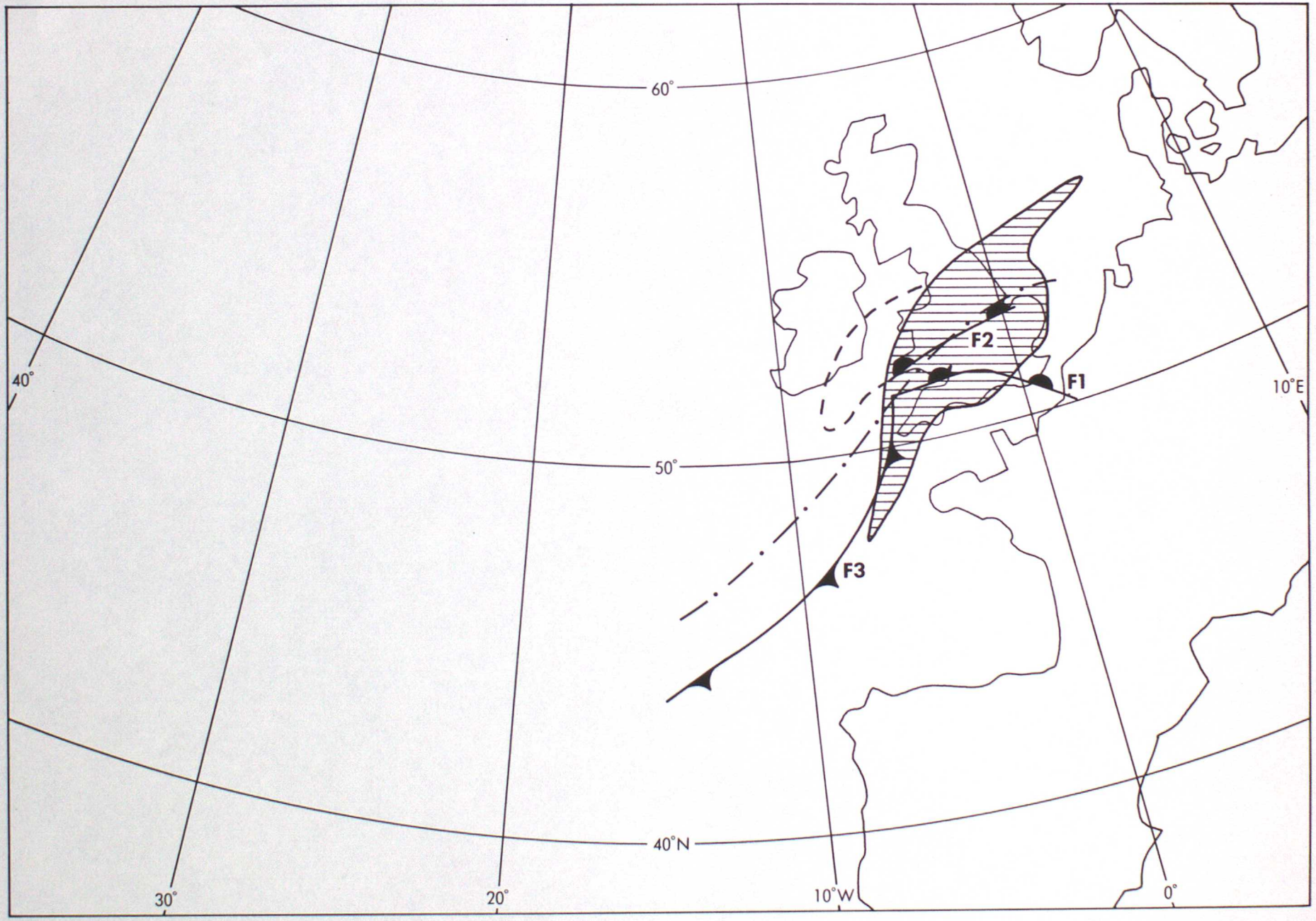

Figure 9b 06Z 20 September 1984

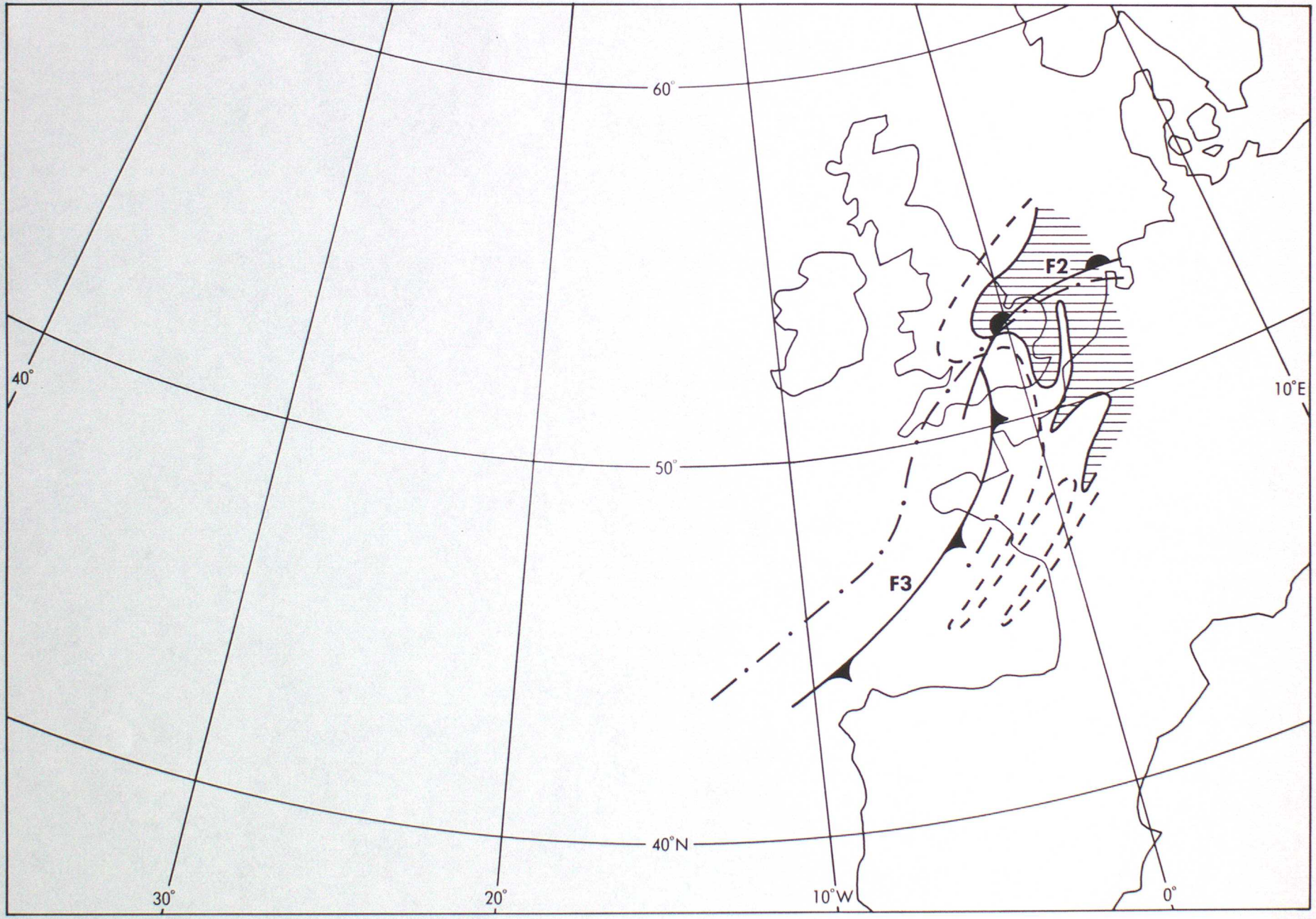

Figure 9c 12Z 20 September 1984

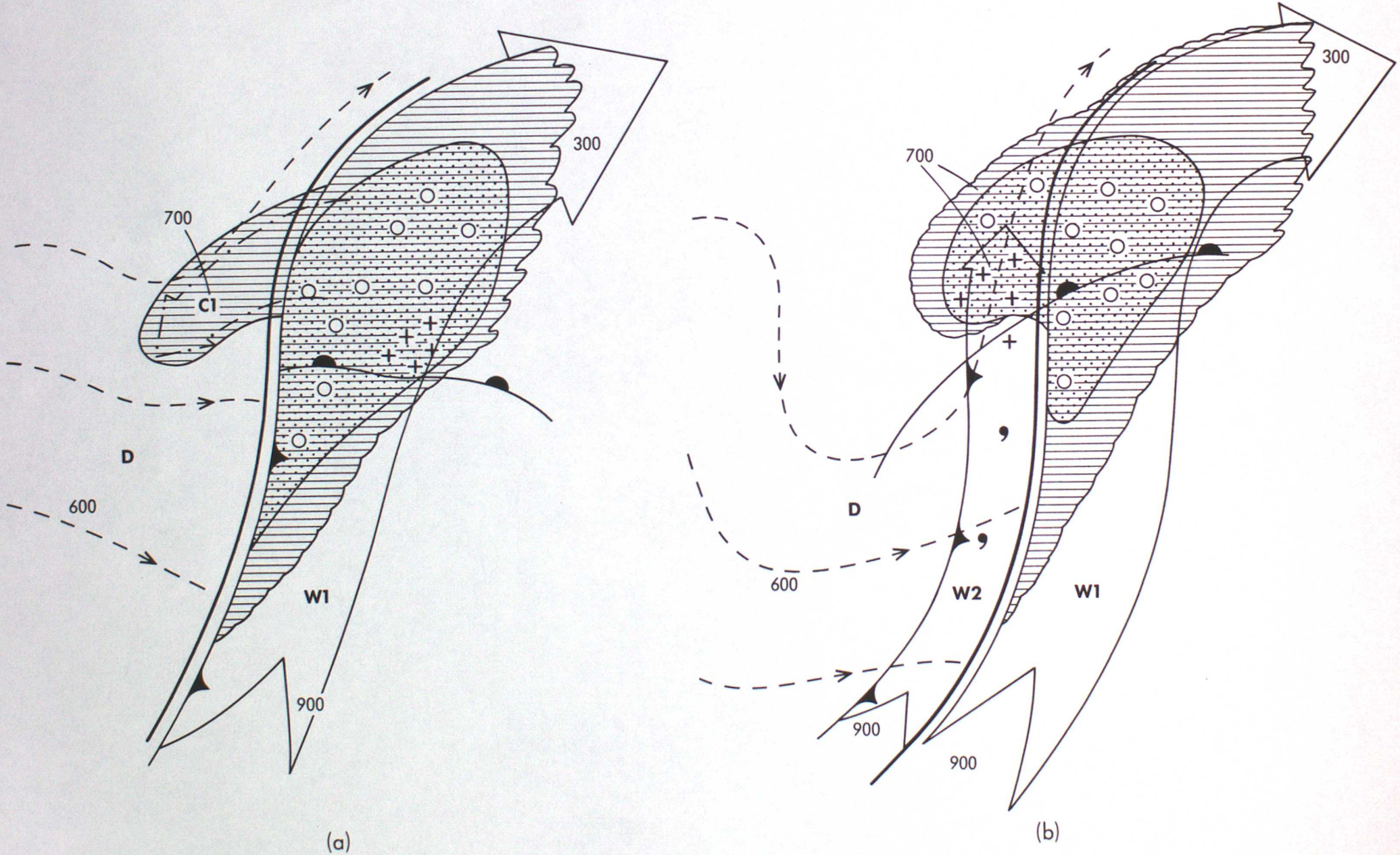

Figure 10